Precise road line localization using single camera and 3D road model

Kiichiro Ishikawa
Takashi Onishi
Yoshiharu Amano
Takumi Hashizume
Waseda University
17 Kikui-cho Shinjyuku-ku Tokyo Japan
ishikawa@power.mech.waseda.ac.jp

Jun-ichi Takiguchi
Shogo Yoneyama

Mitsubishi Electric Corporation
Kamakura Works
325,Kamimachiya,Kamakura-shi,
Kanagawa, Japan
Junichi.Takiguchi@kama.melco.co.jp

Abstract:
In the near future, precise road line location data is said to be applied to car navigation system and ITS to increase the driving safety. It is important to maintain road data freshness and accuracy. A MMS(Mobile Mapping System) can acquire this road database, while offering an unbeatable productivity with the combination of navigation, and videogrammetry tools. The proposed MMS, featuring a GPS/DR(Dead Reckoning) combined navigation system, the 3 axes GPS-Gyro/IMU(Inertial Measurement Unit) , laser scanners, and nearly horizontal cameras, can measure centerline and side-line location precisely considering 3D road surface model based on a laser scanner.

The carrier phased D-GPS/DR combined navigation system and GPS-Gyro/IMU performs highly accurate position and posture estimation at a few centimeter and 0.1 degree order. It can be said that the proposed MMS and its unique road signs positioning method is valid and effective as the road sign location error is within 100[mm] even in the slanted road by considering the 3D road surface model.
Keywords: Mobile Mapping System, GPS- Gyro /IMU, Road line survey, GIS

1. Introduction

The development of road telematics requires the management of continuously growing road databases. For example, car navigation system's road map is revised every four years in Japan. But current market demands more frequent map information updates. If it were executed every two years, it would grow much larger. On the other hand, road maintenance services require the features of the pavement as database. Each road data should be linked to marked or painted points whose position is defined within a linear referencing system or as the absolute coordinates. A MMS can acquire this road database, while offering an unbeatable productivity with the combination of navigation and videogrammetry tools. Our mobile mapping system can be distinguished from its predecessors by its ability to georeference the road signs through vertical oriented camera [1] or nearly horizontal camera with flat road model[2]. The proposed MMS, featuring an excellent GPS/DR combined navigation system, 3 axes GPS-Gyro/IMU, laser scanners, nearly horizontal cameras and high sampling rate road data measurement logger can measure centerline and side-line location precisely considering 3D road surface model.

The carrier phased D-GPS/DR combined navigation system and 3 axes GPS Gyro performs highly accurate position and posture estimation at a few centimeter and 0.1 degree order. It can be said that the proposed MMS and its unique road signs positioning method is valid and effective as the center-line location error is within 100[mm] even in the slanted road by considering the 3D road surface model.

2. System Concifuration

This mobile mapping system combines an accurate positioning by GPS/DR measurements and attitude/heading referencing by carrier phase based GPS Gyro measurements with three progressive scan cameras and three laser scanners as shown in Fig.1. A hybrid car provides 1500 watt continuously for the sensor and computer's electric power without a supplementary battery. An embedded system guarantees the synchronization of navigation data with imagery. The spatial referencing is provided by PAS (Positioning Augmentation Services) system operated by Mitsubishi Electric Corporation. Two GPS antennas are set parallel to the left side of the vehicle and one antenna is set triangular position to the others. The sensor specifications are listed in Table1.

Table1 Sensor Configuration

Loaded sensor	Sensor name	Manufacturer
GPS	BD950	Trimble
	ANTARIS	u-blox
odometer		Mitsubishi Electric
IMU	AHRS400CC-100	Crossbow
Fiber Optic Gyro	JG-35FD	Japan Aviation Electronics
CCD Camera	VGA-120	IMPERX
	2M30C	
	4M15C	
Laser scanner	LMS 291	SICK
	LMS 200	

All sensors are mounted on the top of a van on a rigid roof-rack.

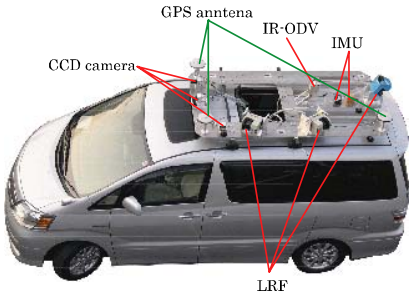

Fig.1. System configuration

3.Precise positioning by GPS/DR measurements and attitude/heading referencing by carrier phase based GPS Gyro/IMU measurements

When operating in higher speeds in quickly changing surroundings, any global application of precise trajectography requires high-performance GPS receivers with instantaneous re-acquisition of signals after loss. The dual frequency receiver Trimble BD950 can provide raw data 10 times per second. To ensure a use of the system under a poor GPS coverage, DR system consisting of an odometer and a FOG(Fiber Optics Gyro) provides the linear speed and angular rate at 120 Hz. The carrier phased D-GPS fixed solution provides aiding to the loosely coupled inertial navigator by EKF(Extended Kalman Filter). Further aiding comes in the form of initial heading angle from the GPS Gyro. The GPS/DR combined navigation system is shown in Fig.2

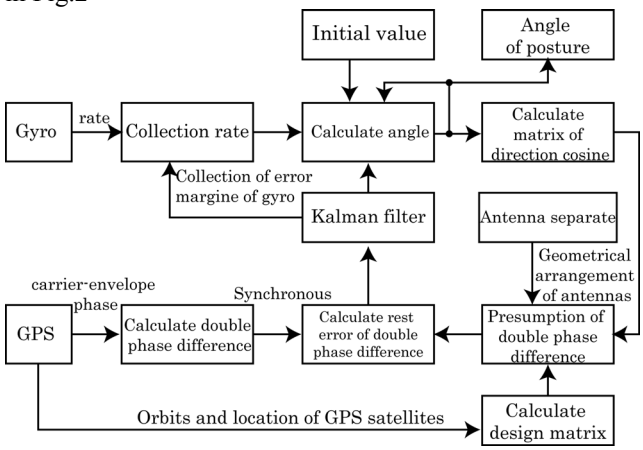

Fig.2. Software synchronized GPS Gyro

The horizontal positioning accuracy is about 20[mm] (1σ) and the vertical one is about 40[mm] (1σ) when excellent GPS visibility is obtained. The GPS Gyro consists of three pairs of single frequency GPS antennas, three un-synchronized receivers, an AHRS providing three angular rates and EKF. As the GPS Gyro's synchronization of three un-synchronized receivers is achieved by the GPS 's UTC time stamp, any low price receivers with low carrier phase noise can be used . The block diagram is shown in Fig.3.

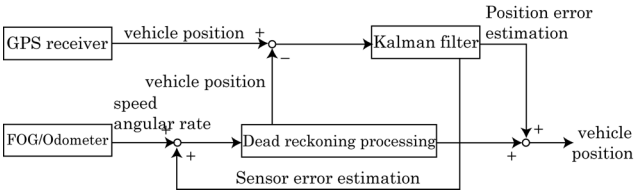

Fig.3. Loosely-Coupled Carrier-Phase D-GPS/DR combined navigation

GPS Gyro's operational theory is shown in Fig.4 Suppose that a and b are GPS antennas which receive same two GPS satellites signal simultaneously.

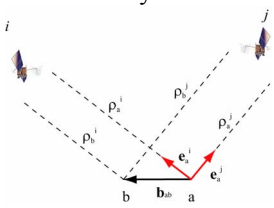

Fig.4. Relation between double difference and baseline vector

The pseudo range ρ_{ab}^{ij} can be expressed as dot product of the baseline vector b_{ab} and its double phase difference as shown in equation (1).

$$\begin{aligned}\rho_{ab}{}^{ji} &= (\rho_b{}^{j} - \rho_a{}^{j}) - (\rho_b{}^{i} - \rho_a{}^{i}) \\ &= -(e_a{}^{j} - e_a{}^{i}) \cdot b_{ab}\end{aligned} \quad (1)$$

Where, b_{ab} is the baseline vector between antenna a and b, $e_a{}^{j}$ is the LOS(Line Of sight) vector from antenna a to satellite j, $e_a{}^{i}$ is the LOS vector from antenna a to satellite i, ρ_b^j is the pseudo range from antenna b to satellite j, ρ_a^j is the pseudo range from antenna a to satellite j, ρ_b^i is the pseudo range from antenna b to satellite i, ρ_a^i is the pseudo range from antenna a to satellite i. Firstly, three independent double phase differences can be obtained by the expansion of the equation (2) to four satellites.

$$\begin{bmatrix}\rho_{ab}{}^{ji} \\ \rho_{ab}{}^{ki} \\ \rho_{ab}{}^{li}\end{bmatrix} = \begin{bmatrix}\lambda(\phi_{ab}{}^{ji} - N_{ab}{}^{ji}) \\ \lambda(\phi_{ab}{}^{ki} - N_{ab}{}^{ki}) \\ \lambda(\phi_{ab}{}^{li} - N_{ab}{}^{li})\end{bmatrix} = \begin{bmatrix}-(e_a{}^{j} - e_a{}^{i}) \\ -(e_a{}^{k} - e_a{}^{i}) \\ -(e_a{}^{l} - e_a{}^{i})\end{bmatrix} b_{ba} \quad (2)$$

Where λ is latitude ϕ is longitude, N is ambiguity. Suppose that all LOS vectors from three un-synchronized receivers are synchronized by the GPS time stamp in the data logger. The Equation (3) is simplified as equation (1) using vector W: double phase differences, A: symmetric positive definite matrix and b: baseline vector.

$$w = Ab \quad (3)$$

Secondly, the baseline vector b in ECEF coordinates can be calculated as equation (6) using Cholesky decomposition.

$$(AA^T)^{-1} = U^T U \quad (4)$$

$$b^T b = w^T U^T U w \quad (5)$$

$$b = Uw \quad (6)$$

Finally the baseline can be calculated with every GPS update epoch as equation (7). The ambiguity N can be calculated by the constraints as shown in (8).

$$\begin{bmatrix} b_1 \\ b_2 \\ b_3 \end{bmatrix} = \begin{bmatrix} u_{11} & u_{12} & u_{13} \\ 0 & u_{22} & u_{23} \\ 0 & 0 & u_{33} \end{bmatrix} \begin{bmatrix} \lambda(\phi_{ab}{}^{ji} - N_{ab}{}^{ji}) \\ \lambda(\phi_{ab}{}^{ki} - N_{ab}{}^{ki}) \\ \lambda(\phi_{ab}{}^{li} - N_{ab}{}^{li}) \end{bmatrix} \quad (7)$$

$$\begin{aligned} -B < b_3 < B \\ -\sqrt{B^2 - b_3{}^2} < b_2 < \sqrt{B^2 - b_3{}^2} \\ -\sqrt{B^2 - (b_3{}^2 + b_2{}^2)} < b_1 < \sqrt{B^2 - (b_3{}^2 + b_2{}^2)} \end{aligned} \quad (8)$$

The coordinates transformation from ECEF to NED is obtained as equation (9), where $C_e{}^n$ is coordinates conversion matrix. Fig.5. shows three antenna placement and its corresponding two baseline vectors: b_2^n and b_3^n.

$$b^n = C_e{}^n b \quad (9)$$

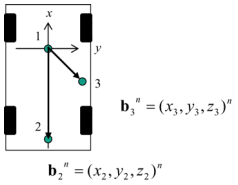

Fig.5. Three antenna placement

Then the vehicle heading and pitching angle is obtained as (10), (11) respectively, and rolling angle is obtained as (12). EKF is used so that an IMU's angle measurement result at 120 Hz is compensated by the GPS Gyro's observation angle.

$$\psi = -\tan^{-1}\left(\frac{x_2}{y_2}\right) \quad (10)$$

$$\theta = \tan^{-1}\left(\frac{z_2}{\sqrt{x_2{}^2 + y_2{}^2}}\right) \quad (11)$$

$$\phi = -\tan^{-1}\left(\frac{z_3''}{x_3''}\right) \quad (12)$$

$$\begin{bmatrix} x_3'' \\ y_3'' \\ z_3'' \end{bmatrix} = \begin{bmatrix} \cos\theta\cos\psi & \cos\theta\sin\psi & -\sin\theta \\ -\sin\psi & \cos\psi & 0 \\ \sin\theta\cos\psi & \sin\theta\sin\psi & \cos\theta \end{bmatrix} \begin{bmatrix} x_3 \\ y_3 \\ z_3 \end{bmatrix} \quad (13)$$

Fig.6 shows the proposed GPS Gyro's angle resolution in a condition that GPS signal which is corresponding to 0 degrees is offered from a GPS simulator(Spirent,GSS7700).

The jerk on the data is caused by the tracked satellite's change. The angle resolution, which is decided by the antenna baseline pitch as well as GPS's L-1 band frequency, is 0.1[deg] for heading and rolling and 0.2[deg] for pitching. The precise posture estimation can contribute to the road sign accuracy improvement as a van tends to cause pitching and rolling movement at larger than 2[deg] in a normal cruise speed. The GPS-Gyro/IMU's measurement angle data which is corresponding to Fig.7's

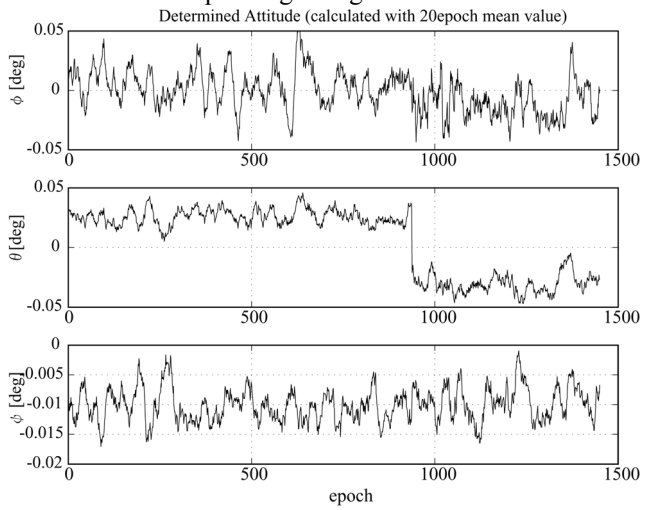

Fig.6. GPS Gyro stationary test result

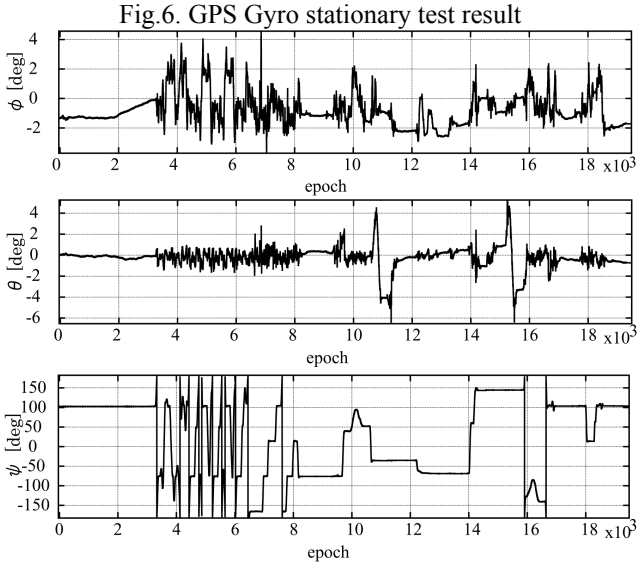

Fig.7. GPS-Gyro/IMU angular measurement result

4. Road line recognition

Road line recognition algorism[18] flow is shown as Fig.8. The Canny filter is used as edge extraction filter.

Horizontal line scanning is used as segmentation. Robustness toward occlusion or "Dash line" is accomplished by various examination processes as shown in Fig.9. Table.2 shows an example of road line detection1 rate.

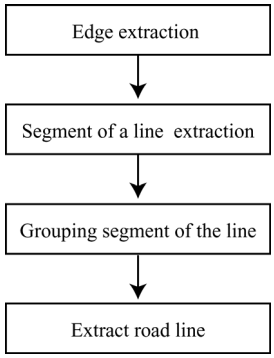

Fig.8. Road line recognition algorism flow

Table2. Road line detection rate

	Detection rate [%]
Video1(4276 frame)	91.3
Video2(9750 frame)	93.7

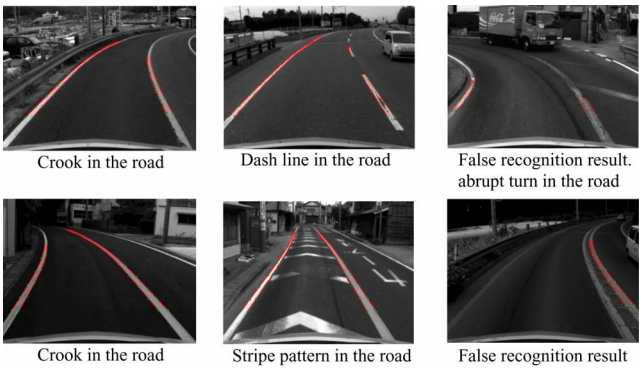

Fig.9. Recognition result

5. White line localization

The proposed MMS, featuring an excellent GPS/DR combined navigation system, a GPS-Gyro/IMU, a laser scanner and high sampling rate road data measurement logger, can measure centerline and side-line location precisely considering 3D road surface model based on the laser scanner's range data. Firstly, the point-clouds data obtained by a laser scanner which is mounted vertically to road surface is converted to NEU orthogonal coordinates by the posture and the position considering the van's body coordinate and sensor coordinate. Suppose that r,θ_{LRF} is laser scanner's range raw data and $\mathrm{N_V},\mathrm{U_V},\mathrm{E_V}$ is the vehicle position. The coordinates transformation is shown in the equation (14).

$$\begin{bmatrix} N_{LRF} \\ U_{LRF} \\ E_{LRF} \\ W_{LRF} \end{bmatrix} = T(N_V,U_V,E_V)R_x(\phi_V)R_z(\theta_V)R_y(\psi_V) \quad (14)$$

$$T(\Delta x_{LRF},\Delta y_{LRF},\Delta z_{LRF})R_x(\phi_{LRF})R_z(\theta_{LRF})R_y(\psi_{LRF})\begin{bmatrix} x_{LRF} \\ y_{LRF} \\ 0 \\ 1 \end{bmatrix}$$

$$\begin{bmatrix} x_{LRF} \\ y_{LRF} \end{bmatrix} = r\begin{bmatrix} \cos\theta_{LRF} \\ \sin\theta_{LRF} \end{bmatrix} \quad (15)$$

$\Delta \mathrm{x_{LRF}},\Delta \mathrm{y_{LRF}},\Delta \mathrm{z_{LRF}}$ is the distance between the GPS antenna position and the laser scanner position, , ϕ_V is the vehicle roll angle, θ_V is the vehicle pitch angle, ψ_V is the vehicle yaw angle, and $\phi_{LRF},\theta_{LRF},\psi_{LRF}$ is the laser scanner's mounting angle toward the body flame. Fig.10 shows an obtained point-cloud data in NEU coordinates and Fig.9 shows the corresponding image data with road symbol recognition result. The obtained 3D data has sufficient resolution so that it can identify sidewalk's edge. Fig.10 shows the white line image processing procedure. The white line position on the camera's u-v coordinates is calculated and recorded as representative points along with the edges as shown in Fig.10. Then, these green points are projected to the corresponding points on 3D road surface model using the camera's LOS(Line Of Sight). Suppose that $\mathrm{N_L},\mathrm{U_L},\mathrm{E_L}$ is the white line position on the image in NEU coordinates. $\mathrm{U_L},\mathrm{V_L}$ is the white line position on the camera image. The camera LOS is obtained in the equation (22).

$$\begin{bmatrix} \mathrm{N_L} \\ \mathrm{U_L} \\ \mathrm{E_L} \\ \mathrm{W} \end{bmatrix} = T(\mathrm{N_V},\mathrm{U_V},\mathrm{E_V})R_x(\phi_V)R_z(\theta_V)R_y(\psi_V) \quad (20)$$

$$T(\Delta \mathrm{x_{cam}},\Delta \mathrm{y_{cam}},\Delta \mathrm{z_{cam}})R_x(\phi_{cam})R_z(\theta_{cam})R_y(\psi_{cam})\begin{bmatrix} \mathrm{U'_L} \\ \mathrm{V'_L} \\ \mathrm{f} \\ 1 \end{bmatrix}$$

$$\begin{bmatrix} \mathrm{U'_L} \\ \mathrm{V'_L} \\ \mathrm{f} \\ 1 \end{bmatrix} = \begin{bmatrix} (\mathrm{U_L}-\mathrm{U\_SIZE}/2)\times \mathrm{Pixel\_SIZE} \\ (\mathrm{V\_SIZE}/2-\mathrm{V_L})\times \mathrm{Pixel\_SIZE} \\ \mathrm{f} \\ 1 \end{bmatrix} \quad (21)$$

Where, $R_x(\phi)$ is rotating matrix around x-axis, $R_Y(\phi)$ is rotating matrix around y-axis, $R_Z(\phi)$ is rotating matrix around z-axis, $T(\mathrm{x},\mathrm{y},\mathrm{z})$ is translation matrix.

$\Delta \mathrm{x_{cam}},\Delta \mathrm{y_{cam}},\Delta \mathrm{z_{cam}}$ is the camera mounting position and $\phi_{cam},\theta_{cam},\psi_{cam}$ is the camera mounting angle.

f is focus of the camera. V_SIZE is vertical resolution. U_SIZE is horizontal resolution. Pixel_SIZE is the camera's CCD size.

$$\frac{\mathrm{x}-\mathrm{N_{cam0}}}{\lambda} = \frac{\mathrm{y}-\mathrm{U_{cam0}}}{\mu} = \frac{\mathrm{z}-\mathrm{E_{cam0}}}{\upsilon} \quad (22)$$

Where, $\mathrm{N_{cam0}}$ $\mathrm{U_{cam0}}$ $\mathrm{E_{cam0}}$ is Camera center position.

$$\lambda = \frac{\mathrm{N_L}-\mathrm{N_{cam0}}}{\sqrt{(\mathrm{N_L}-\mathrm{N_{cam0}})^2+(\mathrm{U_L}-\mathrm{U_{cam0}})^2+(\mathrm{E_L}-E_{cam0})^2}} \quad (23)$$

$$\mu = \frac{\mathrm{U_L}-\mathrm{U_{cam0}}}{\sqrt{(\mathrm{N_L}-\mathrm{N_{cam0}})^2+(\mathrm{U_L}-\mathrm{U_{cam0}})^2+(\mathrm{E_L}-E_{cam0})^2}} \quad (24)$$

$$\upsilon = \frac{\mathrm{E_L}-E_{cam0}}{\sqrt{(\mathrm{N_L}-\mathrm{N_{cam0}})^2+(\mathrm{U_L}-\mathrm{U_{cam0}})^2+(\mathrm{E_L}-E_{cam0})^2}} \quad (25)$$

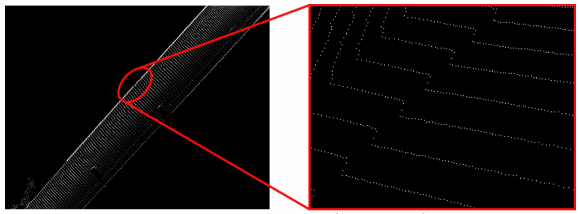

Fig.10. Point cloud road model

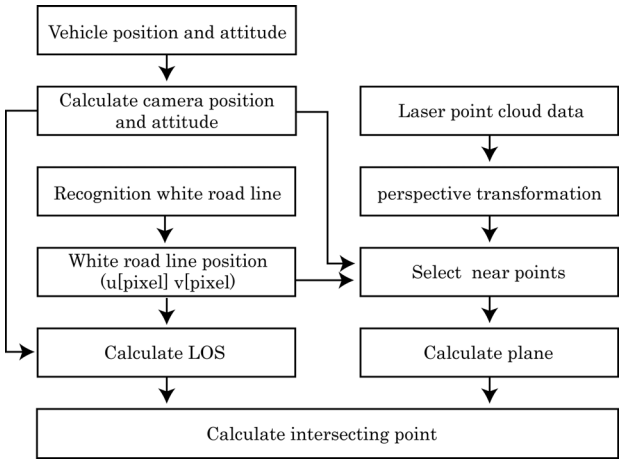

Fig.11. White road line localization algorithm

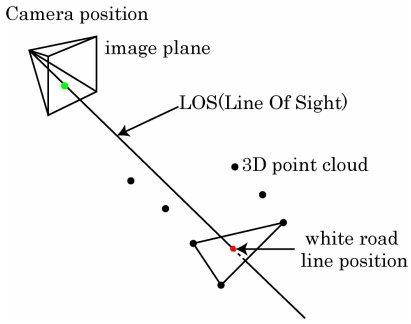

Fig.12. White road line localization

Fig.12 shows the image projection to the 3D road surface algorithm. The closest 3 points on the 3D road surface where their aspect intersects the LOS is chosen as corresponding polygon. Hence, the representative point on the polygon is calculated as a gravity point of these three points in ENU coordinates. In order to check the proposed method, point-cloud data on the road surface model is projected to the camera's u-v coordinates adversely. An example of this reverse perspective transformation result is depicted in Fig.13. Green points represent the transformed point-cloud data on the road surface model. It can be said that the proposed method as well as camera parameter identification is valid as the sidewalk's edge on the image is correctly corresponding to that of point-cloud data on the road surface model.

Thus, the textured 3D point cloud model can be obtained as shown in Fig.14. Fig.15 is the corresponding road line localization result. It can be said that precise 3D reconstruction is achieved by the proposed method. Fig.15 shows the measurement point and Fig.17 shows its localization result. The total-station's result is treated as true. It can be said that the proposed MMS and its unique road signs positioning method is valid and effective as the center-line location error is within 100[mm] even in the slanted road by considering the 3D road surface model.

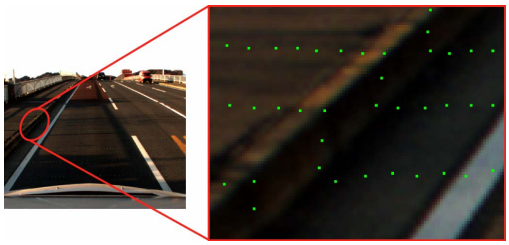

Fig.13. Perspective transformation result

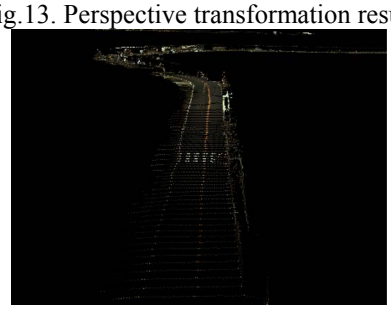

Fig.14. Textured 3D point cloud model

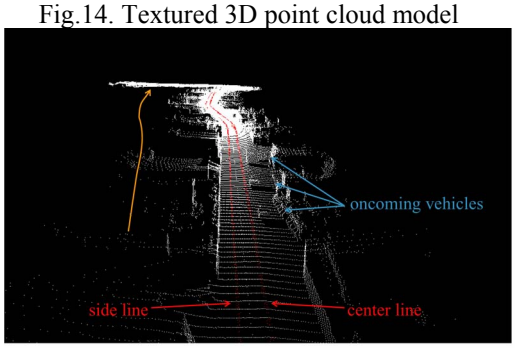

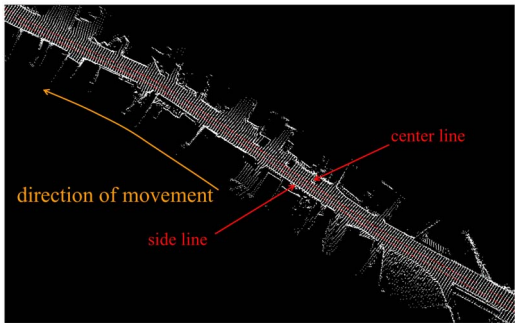

Fig.15. White road line localization result

6. Conclusion

The proposed MMS can acquire this road database, While offering an unbeatable productivity with the combination of navigation, high-resolution images and laser-based range information. The MMS, featuring a GPS/DR combined navigation system, a GPS-Gyro/IMU, nearly horizontal cameras, laser scanners and high sampling rate road data measurement logger, can measure centerline and side-line location precisely considering 3D road surface model. The carrier phased D-GPS/DR combined navigation system and GPS-Gyro/IMU performs highly accurate position and posture estimation at a few centimeter, 0.1 [deg] for heading and pitching, and 0.2[deg] for rolling. Thus, the system allows within 100 [mm] resistitution of both centerline and side-line when GPS's fix solution is obtained.

This MMS's road symbol recognition ability will be used as road maintenance database for road pavement maintenance as well as geographical information for car navigation.

Fig.16. White road line localization accuracy evaluation test Environment

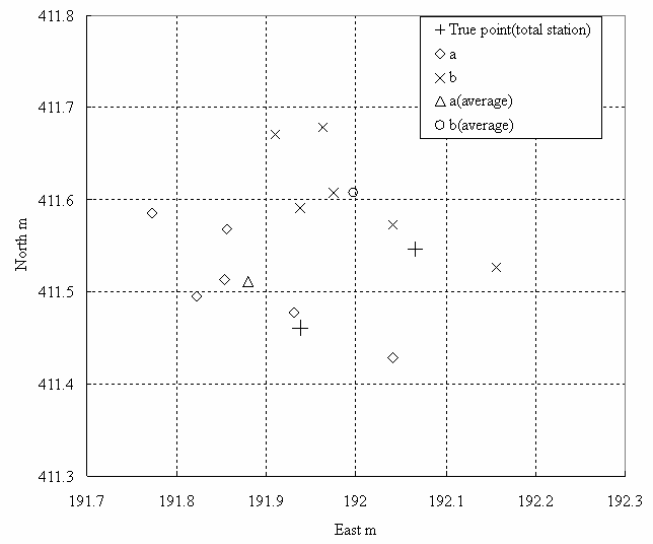

Fig.17. White road line localization accuracy evaluation result

REFERENCES

[1] Dorota A. Grejner-Brzezinska, Charles Toth,"High Accuracy Dynamic Highway Mapping Using a GPS/INS/CCD System with On-The-Fly GPS Ambiguity Resolution",GISS Users Manual Version 2.0, 2004

[2] H. Gontran, J. Skaloud, P. –Y. Gillieron,"AMOBILE MAPPING SYSTEM FOR ROAD DATA CAPTURE VIA A SINGLE CAMERA", 6th optical 3D Measurement Techniques - Zurich, Switzerland, 2003.

[3] Hujing Zhao, Ryosuke Shibasaki,"Reconstructing a textured CAD model an urban environment using vehicle-borne laser range scanners and line cameras.", Machine Vision and Applications, pp.35-41,2003

[4] Dinesh Hanandhar, Ryosuke Shibasaki, "VEHICLE-BORNE LASER MAPPING SYSTEM (VLMS) FOR 3-D GIS", Geoscience and Remote Sensing Symposium, 2001. IGARSS '01. IEEE 2001 International, pp.2073-2075, 2001

[5] Christian Frueh, Siddharth Jain Avideh Zakhor "Data Processing Algorithms for Generating Textured 3D Building Façade Meshes from Laser Scans and Camera Images", International Journal of Computer Vision 64(2), pp.159-184,2005

[6] C. Vincent Tao, "Mobile Mapping Technology for Road Network Data Acquisition" , Proc. Journal of Geospatial Engineering, vol.2, No.2, pp.1-13,2000

[7] Jay A. Farrel, Mattew Barth, "The Global Positioning System and Inertial Navigation", McGrawHill, pp 142-146, 1999

[8] Grang Lu, "Development of a GPS Multi-Antenna System for Attitude Determination", University of Calgray, 1995

[9] Chaochao Wang, Development of a Low-cost GPS-based Attitude Determination System, University of Calgary, 2003

[10] B.Hofmann-Wellenhof, H. Lichtenegger, J. Collins, "GPS Third edition", Springer-Verlag Wien New York, 1994

[11] Jonathan, P. Bernick, "COMPUTATIONAL ANALYSIS OF GPS UDSRAIM ALGORITHMS NEW MEXICO INSTITUTE OF MINING AND TECHNOLOGY", Ph.D. Dissertation at New Mexico Institute of Mining and Technology, 1998

[12] N. El-Sheimy, K. P. Schwarz, "Kinematic Positioning in Three Dimensions Using CCD Technology" IEEE Vehicle Nabigation & Information Systemss Conference, Ottawa VNIS'93, pp472-475 1993

[13] Paul D. Kelly, Gordon Dodds, "Landmark Integration Using GIS and Image Processing for Environmental Analysis with Outdoor Mobile Robots", Conference on Intelligent Robots and Systems, Las Vegas, Nevada,pp,2980-2985, 2003

[14] Diebolt Frank, "ROAD MARKINGS RECOGNITION", Image Processing, pp. 669-672,1996

[15] G. Piccioli, E. De Micheli, P. Parodi, M.Campani, "Robust road sign detection and recognition from image sequences", Intelligent Vehicles' 94 Symposium, pp.278-283, 1994

[16] S. BEUCHER, X.YU, "ROAD RECOGNITION IN COMPLEX TRAFFIC SITUATIONS", 7th IFAC/IFORS Symposium on Transportation Systems, pp. 413-418, 1994

[17] Iyad Abuhadrous, Samer Ammoun, Fawzi Nashashibi, Francois Goulette, Glaud Laurgeau, "Digitizing and 3D Modeling of Urban Environments and Roads using Vehicle-Borne Laser Scanner System", IEEE/RSJ International Conference on Intelligent Robots and Systems,pp.76-81,2004

[18] R. Hirokawa, et al, "Autonomous Vehicle Navigation with Carrier Phase DGPS and Laser-Scanner Augmentation", ION GNSS 2004, pp1115-1123, 2004

[19] Shogo Yoneyama, et al, "An Examination of The Detection of Road Line and Crosswalk Using Road Structure Information" FIT2004, pp.193-194,2004